

# Ultrashort-pulse-pumped, single-mode type-0 squeezers in lithium niobate nanophotonics

Martin Houde<sup>1</sup>, Liam Beaudoin<sup>2</sup>, Kazuki Hirota<sup>2,4</sup>,  
Rajveer Nehra<sup>2,3†</sup>, and Nicolás Quesada<sup>1\*</sup>

<sup>1</sup> Department of Engineering Physics,

École Polytechnique de Montréal, Montréal, Québec, H3T 1J4, Canada

<sup>2</sup>Departments of Electrical and Computer Engineering,

University of Massachusetts Amherst, Amherst, Massachusetts 01003, USA

<sup>3</sup>Departments of Physics,

University of Massachusetts Amherst, Amherst, Massachusetts 01003, USA

<sup>4</sup>Department of Applied Physics,

The University of Tokyo, 7-3-1 Hongo, Bunkyo-ku, Tokyo 113-8656, Japan

To whom correspondence should be addressed;

E-mail: <sup>†</sup>rajveernehra@umass.edu, \*nicolas.quesada@polymtl.ca

**We present design principles for ultrashort-pulse, type-0 phase-matched optical parametric amplifiers to generate and measure spectrally pure degenerate squeezed light. We achieve a Schmidt number of  $K \approx 1.02$  with squeezing levels greater than 15 dB spanning over  $> 5$  THz bandwidth with cm-scale devices on thin-film lithium niobate (TFLN) on insulator platform. Our work opens up promising avenues for large-scale circuits for ultrafast quantum information processing and quantum sensing applications on rapidly advancing TFLN platform with already demonstrated linear components and photodetection capabilities.**

# Introduction

Integrated photonics is a platform for scalable quantum information systems (QISs) (1–3). A building block for photonic quantum technologies is a squeezed light source that meets the following criteria (4): (i) Integration of multiple identical, coherent, and stabilized sources for complex quantum circuits, (ii) Squeezed light in a consistent single spatiotemporal mode across various squeezing levels, eliminating narrow-band filters, (iii) Squeezing levels and bandwidth enabling quantum advantage in information processing, sensing, and metrology, and (iv) Compatibility with ultra-broadband fields and photon counting measurements.

Integrated squeezed light sources using spontaneous four-wave mixing  $\chi^{(3)}$  in SiN and silica resonators (4) address desiderata (i–iv) but require precise filtering and locking due to proximity of pump-signal resonance and frequency sensitivity to thermal fluctuations. On the other hand, single-pass squeezers based on phase-sensitive optical parametric amplifiers (OPAs) utilizing stronger second-order optical nonlinearity  $\chi^{(2)}$  have been proposed and demonstrated in continuous-wave (CW) and pulsed regimes (5–7). In such OPAs, the spontaneous parametric downconversion (SPDC) process allows the signal photons to be emitted across multiple modes governed by the pump profile and phase-matching conditions. Ultrashort-pulsed pump OPAs, in particular, produce photons across numerous spatiotemporal modes, which reduces the quantum state purity for single-photon and squeezed light generation applications. While spectrally de-correlated single-mode operation is achievable in non-degenerate type-II twin-beam squeezing through careful design (7–9), the design principles for single-mode degenerate squeezing with type-0 SPDC sources remain undeveloped. Although twin-beam squeezing can, in principle, be converted to degenerate squeezed modes using linear optics (e.g., beam splitters and mode converters), this approach introduces additional losses and complexities, failing to meet i–iii.

Here, we introduce design principles for ultrashort-pulse-pumped, near-single spatiotemporal mode traveling-wave squeezers using type-0 phase matching, engineered through the group velocity and group velocity dispersion of the relevant modes in rapidly emerging thin-film lithium niobate platform. In the low gain, “pair limit”, we achieve a Schmidt number of  $K \approx 1.115$  for a 50 fs pump and generate squeezing over  $> 5$  THz bandwidth. Additionally, we demonstrate the efficacy of these OPAs in the high-gain regime for all-optical, loss-tolerant, ultra-broadband quadrature measurements, achieving near-unity fidelity between the high-gain measurement OPA (MOPA) mode and the system (squeezer OPA + MOPA). Our designs satisfy desiderata (*i-iv*), thereby paving a practical path for QISs for ultrafast information processing and sensing applications.

## Design principles

The squeezed state wavefunction is  $|\text{sq}[J]\rangle = \exp\left(\frac{1}{2} \int d\omega d\omega' [J(\omega, \omega') a^\dagger(\omega) a^\dagger(\omega') - \text{h.c.}]\right) |0\rangle$ . Here,  $|0\rangle$  is the vacuum state,  $a^\dagger(\omega)/a(\omega)$  are bosonic creation/annihilation operators,  $J(\omega, \omega') = J(\omega', \omega)$  is the symmetric joint spectral amplitude (JSA) defining  $|\text{sq}[J]\rangle$ , “h.c.” denotes the Hermitian conjugate, and integration spans positive frequencies. Spectral separability requires  $J(\omega, \omega')|_{\text{separable}} = r f(\omega) f(\omega')$  where  $f(\omega)$  is  $L^2$  normalized and  $r$  is the squeezing parameter, i.e.,  $10 \log_{10} e^{2r}$  dB squeezing. Requirements (*i-ii*) mathematically translate to a separable JSA at varying squeezing levels for a given frequency mode  $f(\omega)$ . The Schmidt number characterizes the single-modeness of the state, defined as

$$K[J] = \left[ \sum_k \sinh^2 r_k \right]^2 / \sum_k \sinh^4 r_k, \quad (1)$$

where the squeezing parameters are obtained by writing the Takagi (*10*) decomposition  $J(\omega, \omega') = \sum_k r_k f_k(\omega) f_k(\omega')$ , with  $K = 1$ , implying  $r_k = r \delta_{k,0}$  and indicating a single-mode source.

In writing the expression for  $|\text{sq}[J]\rangle$  we are assuming that the transverse degrees of freedom are controlled by the waveguide and that no other waveguided modes are phase-matched (which we confirm numerically in Fig. 1f). Hence, as we will show, our design achieves a single spatiotemporal mode (11).

In type-0 configuration with second harmonic pump (P,  $2\bar{\omega}$ ) and fundamental harmonic signal (S,  $\bar{\omega}$ ) modes, the JSA for nearly single-mode  $< 10$  dB squeezing is:  $J(\omega, \omega') = C\alpha(\omega + \omega' - 2\bar{\omega})\text{sinc}\frac{\Delta k(\omega, \omega')\ell}{2}$  where  $\alpha(\omega - 2\bar{\omega})$  is the pump amplitude and  $\ell$  is the OPA length. The phase-mismatch  $\Delta k(\omega, \omega') = -k_P(\omega' + \omega) + k_S(\omega) + k_S(\omega')$  can then be simplified using dispersion relations as,

$$\begin{aligned} \Delta k(\omega, \omega') = & -\bar{k}_P - \frac{1}{v_P}(\delta\omega + \delta\omega') - \frac{1}{2}\beta_P(\delta\omega + \delta\omega')^2 \\ & + 2\bar{k}_S + \frac{1}{v_S}(\delta\omega + \delta\omega') + \frac{1}{2}\beta_S[(\delta\omega)^2 + (\delta\omega')^2], \end{aligned} \quad (2)$$

where  $\delta\omega = \omega - \bar{\omega}_S$  and  $\beta_S/\beta_P$  are the group velocity dispersion (GVD)w terms. We will assume zeroth order phase-matching ( $2\bar{k}_S - \bar{k}_p = 0$  or  $\pm 2\pi/\Lambda$  if poling with period  $\Lambda$  is used for quasi-phasematching). When the group velocity matching (GVM) condition  $v_P \approx v_S$  is satisfied and  $\beta_S \gg \beta_P$ , the characteristic bandwidth of the PMF  $\sqrt{\beta_S L}$  is much smaller than the pump bandwidth, resulting in

$$J(\omega, \omega') \approx C'\text{sinc}\frac{\ell\beta_S}{4}[(\delta\omega)^2 + (\delta\omega')^2], \quad (3)$$

which excellently approximates a separable function in its two arguments. While the design principle described above is only valid in the low-gain regime, we perform quantum-nonlinear optical simulations (12) of the problem at arbitrary gain verifying the near-single modeness of the source, showing that indeed its does not degrade (in fact it improves) as one increases the gain. This is shown in Fig.1.c.

## Lithium niobate nanophotonics

We design OPAs on the emerging thin-film lithium niobate on insulator platform (6, 13), shown in Fig. 1a. In recent years, thin-film lithium niobate (TFLN) on insulator has emerged as a promising platform to address these outstanding challenges in quantum nanophotonics (14–16). In TFLN, the synergy of sub-wavelength mode confinement, strong second-order ( $\chi^{(2)}$ ) optical nonlinearity, efficient quasi-phase-matching (QPM) through periodic poling, and dispersion engineering for prolonged spatiotemporal confinement has led to devices outperforming traditional bulk LN devices by more than an order of magnitude in nonlinear efficiency and bandwidth. The stronger ( $\chi^{(2)}$ ) allows one for single-pass traveling-wave nonlinear quantum device waveguides, circumventing technical challenges in high-Q resonators (6, 17–20). Moreover, larger electro-optic coefficients in TFLN have enabled electro-optic modulators (EOMs) with a bandwidth exceeding 100 GHz, reduced  $V_\pi$  voltage, and a small device footprint for large-scale programmable interferometers (21).

Considering fundamental signal and SH modes at 2090 nm and 1045 nm (mode profiles in Fig. 1a) with a 700 nm thin-film thickness and  $\theta = 70^\circ$  ridge angle, we find optimal parameters: etching depth  $d = 517.7$  nm and top width  $w = 942.3$  nm through numerical simulations (22). These satisfy GVM ( $v_P - v_S \simeq 0$ ) and GVD ( $\beta_S = 650$  fs<sup>2</sup>/mm  $\gg$   $\beta_P = 50$  fs<sup>2</sup>/mm) conditions for a 50 fs SH pump and 10-mm-long device.

Fig. 1b shows the JSI for 18 dB squeezing, with the inset displaying the SH pump profile, achieving near-separability (Schmidt number  $K \sim 1$ ). Fig. 1c depicts  $K$ 's dependence on signal photon numbers, spanning single photon pair generation (SPG) to high squeezing, with the inset showing the JSI in the SPG regime. Note that the Schmidt number could be further reduced with aperiodic poling (23). Fig. 1d shows the mode fractions at 18 dB gain (inset: SPF regime), with a first/second mode ratio of 0.989/0.00687 (0.947/0.02), demonstrating the

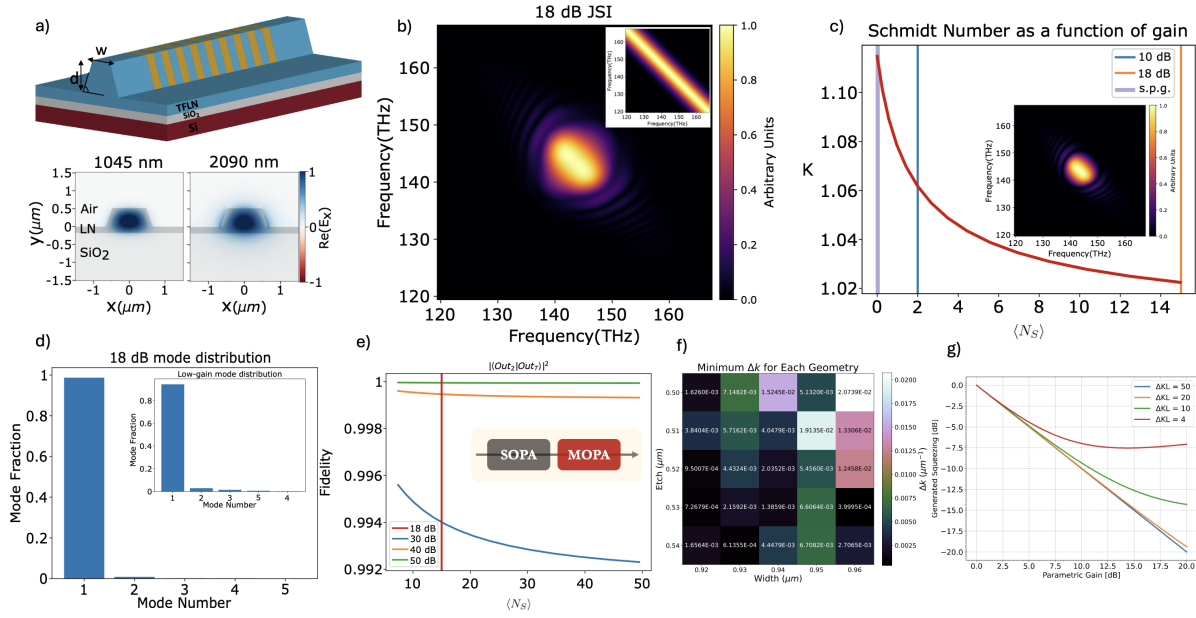


Figure 1: (a) Waveguide design and transverse mode profiles for SH and FH modes in lithium niobate nanophotonics. (b) Joint spectral intensity (JSI) in the high-gain regime (18 dB gain) with pump spectral amplitude for a 50 fs pulse (inset). (c) Schmidt number,  $K$ , as a function of average signal photons  $\langle N_S \rangle$ , inset: JSI for single photon pair generation regime. (d) Mode distribution in the high-gain regime (inset: low-gain). (e) Fidelity between the MOPA output state and the system output state. (f) Calculated phase mismatch,  $\Delta k$ , for varying depth and width. (g) Squeezing degradation due to noise contamination from undesired modes.

versatility of our design for both single-photon and squeezed light generation.

We next show the efficacy of our OPAs in the high-gain regime as a measurement device, for conducting the recently emerging all-optical, loss-tolerant measurements over  $> 5$  THz bandwidth (6, 24–27). The entire system consists of a squeezer OPA (SOPA) and a high-gain measurement OPA (MOPA), as shown in the inset of Fig. 1e. In multi-mode systems, the modes can mix, leading to output Schmidt modes for the total system that may differ from the MOPA modes, thereby degrading the measurement quality. We define the fidelity between the frequency profiles of two spatiotemporal modes as

$$F(f_i, f_j) = \left| \int d\omega f_i(\omega) (f_j(\omega))^* \right|^2. \quad (4)$$

We can describe a system of two cascaded squeezers, such as a SOPA (squeezer OPA) followed by a MOPA (amplifier OPA), using three different sets of input/output Schmidt modes: one set for each stage (SOPA modes and MOPA modes) and a third set representing the overall interaction. The MOPA serves as an anti-squeezer and typically operates with significantly higher gain than the SOPA. The output modes for the total interaction should match the output modes of the MOPA for high-fidelity measurements.

In the quadrature basis, we can describe the evolution through different nonlinear media via real-symplectic matrices  $\mathbf{S}_{SOPA}$ ,  $\mathbf{S}_{MOPA}$ , and  $\mathbf{S}_T = \mathbf{S}_{MOPA}\mathbf{S}_{SOPA}$ . These are the Heisenberg propagators for a given nonlinear region. Using the Bloch-Messiah decomposition, we can break these propagators into terms which explicitly tell us about the input and output Schmidt modes

$$\mathbf{S}_{SOPA} = \mathbf{O}_{SOPA}\mathbf{\Lambda}_{SOPA}\tilde{\mathbf{O}}_{SOPA}^T \quad (5)$$

$$\mathbf{S}_{MOPA} = \mathbf{O}_{MOPA}\mathbf{\Lambda}_{MOPA}\tilde{\mathbf{O}}_{MOPA}^T \quad (6)$$

$$\mathbf{S}_T = \mathbf{O}_T\mathbf{\Lambda}_T\tilde{\mathbf{O}}_T^T = \mathbf{O}_{MOPA}\mathbf{\Lambda}_{MOPA}\tilde{\mathbf{O}}_{MOPA}^T\mathbf{O}_{SOPA}\mathbf{\Lambda}_{SOPA}\tilde{\mathbf{O}}_{SOPA}^T, \quad (7)$$

where the  $\mathbf{O}_\mu$ 's tell us about the output Schmidt modes,  $\tilde{\mathbf{O}}_\mu$  tell us about the input Schmidt modes, and  $\mathbf{\Lambda}_\mu$  ( $\mu = SOPA, MOPA, T$ ). Since we are operating the measurement and squeezing OPAs at different levels of gain there is no guarantee that  $\mathbf{O}_T = \mathbf{O}_{MOPA}$ . In multi-mode systems, we expect the modes to mix together (*i.e.*  $\tilde{\mathbf{O}}_{MOPA}^T \mathbf{O}_{SOPA} \neq \mathbf{1}$ ) potentially giving rise to output Schmidt modes for the total system which could be vastly different than those of the measurement OPA.

In Fig. 1e, we show the fidelity between the output Schmidt modes of the total interaction and those of the MOPA. As demonstrated, for various gain levels in both the measurement OPA and the squeezer OPA, the fidelity remains above 0.99. This indicates that, to a good approximation, the output modes of the total system are those of the measurement OPA.

Careful attention to spatial modes is essential to minimize thermal noise from unwanted parametric interactions. For instance, generating two-mode squeezing (TMS) between the fundamental transverse electric (TE) and transverse magnetic (TM) modes, alongside the desired single-mode squeezing in the fundamental TE mode, can introduce thermal noise via the TMS-TE mode, reducing overall squeezing levels (28). We mitigate this by maximizing parametric gain in the desired modes while avoiding mode matching for unwanted interactions. We calculate the phase mismatch,  $\Delta k_{ijk} = (k_{2\omega,i} - k_{\omega,j} - k_{\omega,k}) - (k_{2\omega,0} - k_{\omega,0} - k_{\omega,0})$  for a number of waveguide geometries to account for fabrication imperfections. Here  $\Delta k_{0,0,0} = 0$  for a given periodic poling corresponding to a quasi-phase-matched interaction for the fundamental TE modes. Fig. 1f shows the numerically simulated  $\Delta k_{ijk}$  where the solver analyzes the spatial modes at both wavelengths and identifies the worst-case scenario, corresponding to the smallest  $\Delta k$ . Fig. 1g shows the phase mismatch impact on squeezing at varying gain for the fundamental pump mode. Squeezing degrades at gains as low as 3 dB for  $\Delta kl = 4$ . Achieving  $>15$  dB squeezing with cm-scale OPAs requires  $\Delta kl > 20$  ( $\Delta k > 0.002 \mu\text{m}^{-1}$ ), met by our designs.

In summary, we propose dispersion engineering principles for traveling-wave, type-0 phase-



matched OPAs to generate squeezing over a single spatiotemporal mode without auxiliary filtering. In the high-gain regime, we demonstrate how such an OPA enables all-optical, loss-tolerant measurements with near-unity fidelity. We also present concrete device designs on TFLN nanophotonics, a promising platform because of its strong optical nonlinearity and large electro-optic coefficients. Our work will enable large-scale circuits with complex functionalities for all-optical mid-IR quantum information processing, spectroscopy, and sensing applications.

NQ and MH acknowledge support from the Ministère de l'Économie et de l'Innovation du Québec and the Natural Sciences and Engineering Research Council of Canada. This work has been funded by the European Union's Horizon Europe Research and Innovation Programme under agreement 101070700 project MIRAQLS. RN gratefully acknowledges support from the College of Engineering, University of Massachusetts, Amherst, and KH is thankful to Japan Science and Technology (JST) Agency (Moonshot R & D) Grant.

## References and Notes

1. E. Pelucchi, *et al.*, *Nature Reviews Physics* **4**, 194 (2022).
2. J. M. Arrazola, *et al.*, *Nature* **591**, 54 (2021).
3. J. E. Bourassa, *et al.*, *Quantum* **5**, 392 (2021).
4. Z. Vernon, *et al.*, *Phys. Rev. Applied* **12**, 064024 (2019).
5. T. Kashiwazaki, *et al.*, *Applied Physics Letters* **122** (2023).
6. R. Nehra, *et al.*, *Science* **377**, 1333 (2022).
7. N. Quesada, *et al.*, *Phys. Rev. A* **98**, 043813 (2018).
8. M. Houde, N. Quesada, *AVS Quantum Science* **5**, 011404 (2023).

9. M. Houde, N. Quesada, *AVS Quantum Science* **6**, 021402 (2024).
10. M. Houde, W. McCutcheon, N. Quesada, *Canadian Journal of Physics* **102**, 497 (2024).
11. M. Houde, L. Beaudoin, R. Nehra, N. Quesada, *submitted to CLEO: Science and Innovations* (2025).
12. L. Helt, N. Quesada, *Journal of Physics: Photonics* **2**, 035001 (2020).
13. L. Ledezma, *et al.*, *Optica* **9**, 303 (2022).
14. A. Boes, *et al.*, *Science* **379**, eabj4396 (2023).
15. M. G. Vazimali, S. Fathpour, *Advanced Photonics* **4**, 034001 (2022).
16. C. Wang, *et al.*, *Nature* **562**, 101 (2018).
17. A. Rao, *et al.*, *Optics express* **27**, 25920 (2019).
18. L. Ledezma, *et al.*, *Optica* **9**, 303 (2022).
19. Q. Guo, *et al.*, *Nature Photonics* **16**, 625 (2022).
20. M. Jankowski, *et al.*, *Optica* **7**, 40 (2020).
21. F. Arab Juneghani, *et al.*, *Advanced Photonics Research* **4**, 2200216 (2023).
22. L. M. Ledezma, Snow: Simulator for nonlinear optical waveguides, <https://github.com/ledezmaluism/snow> (2024).
23. A. M. Brańczyk, T. C. Ralph, W. Helwig, C. Silberhorn, *New Journal of Physics* **12**, 063001 (2010).
24. N. Takanashi, *et al.*, *Optics Express* **28**, 34916 (2020).

25. Y. Shaked, *et al.*, *Nature communications* **9**, 609 (2018).
26. M. Kalash, M. V. Chekhova, *arXiv:2207.10030* (2022).
27. A. Kawasaki, *et al.*, *Nature Communications* **15**, 9075 (2024).
28. Y. Sano, Y. Taguchi, K. Oguchi, Y. Ozeki, *Journal of the Optical Society of America B* **41**, 183 (2023).